J|A|C|S
ARTICLES

Synthesis, Optical, and Electronic Properties of Soluble Poly-*p*-phenylene Oligomers as Models for Molecular Wires

Moloy Banerjee, Ruchi Shukla, and Rajendra Rathore*

Marquette University, Department of Chemistry, P.O. Box 1881,
Milwaukee, Wisconsin 53201-1881

Received July 2, 2008; E-mail: rajendra.rathore@marquette.edu

---

Abstract: A homologous series of soluble poly-*p*-phenylenes containing up to eight phenylene moieties (**PP$_2$**−**PP$_8$**) with branched *iso*-alkyl (or bis-*n*-alkylmethyl) groups has been synthesized and the structure−property relationship with regards to various optical and electronic properties established. All electronic and optoelectronic properties of poly-*p*-phenylenes followed a 1/*n* relationship (where *n* is number of phenylene moieties) with the increasing number of phenylene moieties. The low-energy electronic transition of the **PP$_2$**−**PP$_7$** cation radicals, generated either by laser-flash photolysis or by chemical oxidation, varied as well according to the inverse (1/*n*) relationship. The observed inverse relationship of all measured electronic and optoelectronic properties against the increasing number of phenylene units in various **PP$_n$**'s, as well as X-ray crystallography of both neutral and a cation-radical salt of a representative tetra-*p*-phenylene oligomer allows us to demonstrate that the effective conjugation length in poly-*p*-phenylenes is, in part, controlled by the increasing number of interactions of ortho hydrogens which may prevent simultaneous planarization of the continuous arrays of a large number of phenylene moieties.

Introduction

Since the discovery of conducting polyacetylenes,[1] the study of π-conjugated organic polymers, such as poly-*p*-phenylenes,[2] polythiophenes,[3] poly-*p*-phenylenevinylenes,[4] polyfluorenes,[5] etc., has attracted considerable attention, owing to their potential applications as functional materials in the emerging areas of molecular electronics and nanotechnology.[6] Of these, poly-*p*-phenylenes (**PP$_n$**) are especially important due to their high conductivity when doped with either n- or p-type dopants,[7] usage as active constituents of blue light emitting diodes,[8] ultraviolet laser dyes,[9] and high thermal and oxidative stability.[10] Unfortunately, a lack of processability of poly-*p*-phenylenes, especially when they are unsubstituted, has hampered their study, as well as the exploitation of their extensive potential for practical applications.[11]

Poly-*p*-phenylenes have been utilized as bridges (or spacers) in the molecular assemblies of electron donor (**D**)-bridge (**B**)-electron acceptor (**A**) (i.e., **D**-**B**-**A**) in order to study the mechanism and distance dependence of electron or hole transport (charge transport, CT).[12] The mechanism of charge transport (CT) in various **D**-**B**-**A** systems is suggested to occur via a combination of highly distance dependent coherent (i.e., super exchange) and weakly distance dependent noncoherent (i.e., hopping) mechanisms.[13] Long poly-*p*-phenylene bridges are believed to display noncoherent charge hopping or wire-like

---

(1) (a) Shirakawa, H.; Louis, E. J.; MacDiarmid, A. G.; Chiang, C. K.; Heeger, A. J. *Chem. Commun.* **1977**, *16*, 578–580. (b) MacDiarmid, A. G. *Angew. Chem., Int. Ed.* **2001**, *40*, 2581–2590.

(2) (a) Wallow, T. I.; Novak, B. N. *J. Am. Chem. Soc.* **1991**, *113*, 7411–7412. (b) Gin, D. G.; Conticello, V. P.; Grubbs, R. H. *J. Am. Chem. Soc.* **1992**, *114*, 3167–3169. (c) Tour, J. M. *Adv. Mater.* **1994**, *6*, 190–198. (d) Berresheim, A. J.; Muller, M.; Mullen, K. *Chem. Rev.* **1999**, *99*, 1747–1785.

(3) (a) Roncali, J. *Chem. Rev.* **1992**, *92*, 711–738. (b) Inganaes, O.; Berggren, M.; Andersson, M. R.; Gustafsson, G.; Hjertberg, T.; Wennerstroem, O.; Dyreklev, P.; Granstroem, M. *Synth. Met.* **1995**, *71*, 2121–2124. (c) McCullough, R. D. *Adv. Mater.* **1998**, *10*, 93–116. (d) *Handbook of Oligo- and Polythiophenes*; Fichou, D., Ed.; Wiley-VCH: Weinheim, Germany, 1999. (e) Bauerle, P.; Mitschke, U.; Gruner, G.; Rimmel, G. *Pure Appl. Chem.* **1999**, *71*, 2153–2160.

(4) (a) Davis, W. B.; Svec, W. A.; Ratner, M. A.; Wasielewski, M. R. *Nature* **1998**, *396*, 60–63. (b) Kraft, A.; Grimsdale, A. C.; Holmes, A. B. *Angew. Chem., Int. Ed.* **1998**, *37*, 402–428. (c) Van Hutten, P. F.; Krasnikov, V. V.; Hadziioannou, G. *Acc. Chem. Res.* **1999**, *32*, 257–265.

(5) (a) Scherf, U.; List, E. J. W. *Adv. Mater.* **2002**, *14*, 477–487. (b) Li, Z. H.; Wong, M. S.; Tao, Y.; Lu, J. *Chem. Eur. J.* **2005**, *11*, 3285–3293. (c) Li, J. Y.; Ziegler, A.; Wegner, G. *Chem. Eur. J.* **2005**, *11*, 4450–4457. (d) Goldsmith, R. H.; Sinks, L. E.; Kelley, R. F.; Betzen, L. J.; Liu, W.; Wiess, E. A.; Ratner, M. A.; Wasielewski, M. R. *Proc. Natl. Acad. Sci. U.S.A.* **2005**, *102*, 3540–3545. (e) Perepichka, I. I.; Perepichka, I. F.; Bryce, M. R.; Palsson, L.-O. *Chem. Commun.* **2005**, 3397−3399.

(6) (a) *Introduction to Molecular Electronics*, Petty, M. C., Bryce, M. R., Bloor, D., Eds.; Oxford Univ. Press: New York, 1995. (b) Gross, M.; Muller, D. C.; Nothofer, H. -G.; Scherf, U.; Neher, D.; Brauchle., C.; Meerholz, K. *Nature* **2000**, *405*, 661–665. (c) Craig, M. R.; Kok, M. M. de; Hofstraat, J. W.; Schenning, A. P. H. J.; Meijer, E. W. *J. Mater. Chem.* **2003**, *13*, 2861–2862. (d) *Organic Electronics*; Klauk, H., Ed.; Wiley-VCH: Weinheim, 2006.

(7) Shacklette, L. W.; Eckhardt, H.; Chance, R. R.; Miller, G. G.; Ivory, D. M.; Baughman, R. H. *J. Chem. Phys.* **1980**, *73*, 4098–4102.

(8) (a) Meghdadi, F.; Tasch, S.; Winkler, B.; Fischer, W.; Stelzer, F.; Leising, G. *Synth. Met.* **1997**, *85(1−3)*, 1441–1442. (b) Baur, J. W.; Kim, S.; Balanda, P. B.; Reynolds, J. R.; Rubner, M. F. *Adv. Mater.* **1998**, *10*, 1452–1455.

(9) Rinke, M.; Gusten., H; Ache, H. J. *J. Phys. Chem.* **1986**, *90*, 2666–2669.

(10) (a) Gale, D. M. *J. Appl. Polym. Sci.* **1978**, *22*, 1971–1976. (b) Irvine, P. A.; Wu, D. C.; Flory, P. J. *J. Chem. Soc., Faraday Trans. 1* **1984**, *80*, 1795–1806. (c) Baker, K. N.; Fratini, A. V.; Resch, T.; Knachel, H. C.; Adams, W. W.; Socci, E. P.; Farmer, B. L. *Polymer* **1993**, *34*, 1571–1587.

(11) Bredas, J.-L.; Beljonne, D.; Coropceanu, V.; Cornil, J. *Chem. Rev.* **2004**, *104*, 4971–5003.

10.1021/ja805102d CCC: $40.75

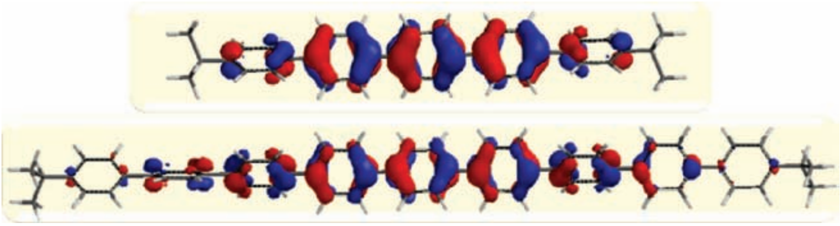

Figure 1. Showing the HOMOs of representative poly-*p*-phenylene derivatives, containing six and nine phenylene moieties, obtained by density functional theory (DFT) calculations at the B3LYP/6-31G* level.

properties.[13] In order to gain a clear distinction between the noncoherent and coherent CT mechanisms operating in these **PP**-based molecular wires, a quantitative understanding as to how the charge is stabilized, or transported, through multiple phenylene moieties that constitute the spacer is desirable.

Although poly-*p*-phenylene-based spacers have been extensively utilized as bridging materials in a variety of **D-B-A** assemblies,[12] even the simplest of their properties, such as redox potentials, of a well-defined series of poly-*p*-phenylenes are not known due to their poor solubility.[14] It is to this effect that we undertook a systematic study to understand the structure−property relationships of such poly-*p*-phenylene oligomers by incorporating solubilizing *iso*-alkyl groups as the end-capping substituents. The end-capping alkyl substitution is expected to have little effect on the electronic properties of such materials, as the HOMO in various poly-*p*-phenylenes gravitates toward the center of the oligomeric chains,[15] i.e., Figure 1.

Accordingly, herein we report the syntheses of a homologous series of soluble poly-*p*-phenylene oligomers (**PP**$_n$) containing up to eight phenylene moieties (i.e., **PP**$_8$) with branched *iso*-alkyl or bis-*n*-alkylmethyl (i.e., 6-tetradecyl) groups as the end capping substituents. The availability of a well-defined series of poly-*p*-phenylenes (**PP**$_2$−**PP**$_7$) allows us to establish, for the first time, the inverse (1/*n*) relationship[16] of the optoelectronic and electrochemical properties of the **PP**$_n$ with the increasing number of phenylene moieties. Moreover, the generation and comparison of the spectral characteristics of the cation radical salts of **PP**$_2$−**PP**$_7$, as well as X-ray crystallographic characterization of a representative cation-radical salt of a quaterphenyl derivative (**PP**$_4$′),[17] allows us to provide a quantitative understanding as to how the cationic charge (or hole) is stabilized by multiple phenylene moieties that constitute the poly-*p*-phenylene polymers. The details of these finding are described herein.

Results and Discussion

Synthesis of Poly-*p*-phenylenes (PP$_n$). In order to obtain the desired **PP**$_n$'s with a defined number of phenylene moieties, we have resorted to the Pd-catalyzed Suzuki reaction, which has emerged as a favored reaction for aryl−aryl bond formation particularly in the synthesis of π-conjugated systems.[18] The starting aryl bromides and the corresponding boronic acids have been synthesized starting from bromobenzene (**1a**) and 4-bromobiphenyl (**1b**) by a sequence of Friedel−Crafts acylation with hexanoyl chloride, Grignard addition to the resulting hexanoylketones (**2a** and **2b**), and a one-pot dehydration and reduction of the tertiary alcohols (**3a** and **3b**) with the borane−dimethyl sulfide complex[19] to form the alkylated bromobenzene (**4a**) and 4-bromobiphenyl (**4b**). The bromo derivatives **4a** and **4b** were easily converted to the corresponding boronic acids (**5a** and **5b**) using a standard literature procedure.[20] The bromoterphenyl derivative (**4c**) was obtained by a selective Suzuki coupling of **5b** with 1-bromo-4-iodobenzene, which in turn was easily converted to the corresponding boronic acid (**5c**) in excellent yield (Scheme 1).

Various combinations of boronic acids [i.e., **5a**−**c** and 1,4-benzenediborate ester (**6**)] and bromo derivatives [i.e., **4a**−**c**, 1,4-dibromobenzene (**7a**), and 4,4′-dibromobiphenyl (**7b**)], obtained in Scheme 1, were then subjected to the Suzuki coupling reactions to afford oligomers **PP**$_2$−**PP**$_8$ in good yields (e.g., see Scheme 2).

It is to be noted that the synthesis of higher oligomers by this iterative approach, in principle, is feasible; however, the solubility of the higher homologues beyond **PP**$_7$ was sharply diminished. For example, **PP**$_6$ has a solubility of ~90 mg/10 mL of dichloromethane, for **PP**$_7$ it is ~45 mg/10 mL, and for **PP**$_8$ it decreased sharply to <1 mg/10 mL of dichloromethane! The structures of readily soluble poly-*p*-phenylene oligomers **PP**$_2$−**PP**$_7$ were delineated by ^{1}H/^{13}C NMR spectroscopy and

---

(12) (a) Weiss, E. A.; Tauber, M. J.; Kelley, R. F.; Ahrens, M. J.; Ratner, M. A.; Wasielewski, M. R. *J. Am. Chem. Soc.* **2005**, *127*, 11842–11850. (b) Plummer, E. A.; Hofstraat, J. W.; De Cola, L. *Dalton Trans.* **2003**, 2080−2084. (c) Weiss, E. A.; Ahrens, M. J.; Sinks, L. E.; Gusev, A. V.; Ratner, M. A.; Wasielewski, M. R. *J. Am. Chem. Soc.* **2004**, *126*, 5577–5584. (d) Welter, S.; Salluce, N.; Benetti, A.; Rot, N.; Belser, P.; Sonar, P.; Grimsdale, A. C.; Mullen, K.; Lutz, M.; Spek, A. L.; De Cola, L. *Inorg. Chem.* **2005**, *44*, 4706–4718. (e) Schlicke, B.; Belser, P.; De Cola, L.; Sabbioni, E.; Balzani, V. *J. Am. Chem. Soc.* **1999**, *121*, 4207–4214. (f) Sun, D.; Lindeman, S. V.; Rathore, R.; Kochi, J. K. *J. Chem. Soc., Perkin Trans. 2* **2001**, 1585–1594. (g) Ward, M. D. *Chem. Soc. Rev.* **1995**, 121−134. (h) Martin, R. E.; Diederich, F. *Angew. Chem., Int. Ed.* **1999**, *38*, 1350–1377.

(13) Dance, Z. E. X.; Mi, Q.; McCamant, D. W.; Ahrens, M. J.; Ratner, M. A.; Wasielewski, M. R. *J. Phys. Chem. B* **2006**, *110*, 25163–25173.

(14) For a cyclic voltammetric study of a limited number of polyphenylenes, see:(a) Meerholz, K.; Heinze, J. *Synth. Met.* **1991**, *42*, 2871–2876. (b) Meerholz, K.; Heinze, J. *Electrochim. Acta* **1996**, *41*, 1839–1854.

(15) (a) Tolbert, L. M. *Acc. Chem. Res.* **1992**, *25*, 561–568. (b) Turker, L. *THEOCHEM* **2002**, *588*, 121–126. (c) Hertel, D.; Setayesh, S.; Nothofer, H.-G.; Scherf, U.; Mullen, K.; Bassler, H. *Adv. Mater.* **2001**, *13*, 65–70.

(16) (a) Rathore, R.; Abdelwahed, S. H.; Guzei, I. A. *J. Am. Chem. Soc.* **2003**, *125*, 8712–8713. (b) Houk, K. N.; Lee, P. S.; Nendel, M. *J. Org. Chem.* **2001**, *66*, 5517–5521. (c) Klaerner, G.; Miller, R. D. *Macromolecules* **1998**, *31*, 2007–2009. (d) Ane′mian, R.; Mulatier, J.-C.; Andraud, C.; Ste′phan, O.; Vial, J.-C. *Chem. Commun.* **2002**, 1608–1609. (e) Scherf, U.; Grimme, J. *Macromol. Chem. Phys.* **1996**, *197*, 2297–2304.

(17) For a preliminary communication, see: Banerjee, M.; Lindeman, S. V.; Rathore, R. *J. Am. Chem. Soc.* **2007**, *129*, 8070−8071, Also note that the repeated attempts to crystallize either the neutral or the cation radical of *iso*-alkyl-substituted **PP**$_4$ were unsuccessful, most likely due to the highly floppy nature of the *iso*-alkyl substituents.

(18) (a) Suzuki, A. *Chem. Commun.* **2005**, 4759–4763. (b) Hassan, J.; Sevignon, M.; Gozzi, C.; Schulz, E.; Lemaire, M. *Chem. Rev.* **2002**, *102*, 1359–1469.

(19) Compare: Rathore, R.; Weigand, U.; Kochi, J. K. *J. Org. Chem.* **1996**, *61*, 5246−5256.

(20) Banerjee, M.; Emond, S. J.; Lindeman, S. V.; Rathore, R. *J. Org. Chem.* **2007**, *72*, 8054–8061.

Scheme 1. Synthesis of Bromo and Boronic Acid Precursors for the Preparation of Various **PP*n***'s

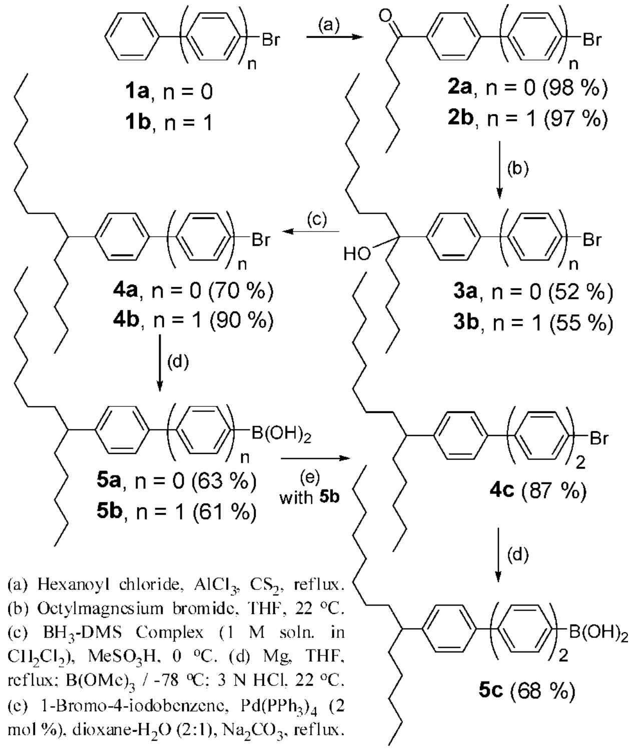

(a) Hexanoyl chloride, $AlCl_3$, CS_2, reflux. (b) Octylmagnesium bromide, THF, 22 °C. (c) BH_3-DMS Complex (1 M soln. in CH_2Cl_2), $MeSO_3H$, 0 °C. (d) Mg, THF, reflux; $B(OMe)_3$ / -78 °C; 3 N HCl, 22 °C. (e) 1-Bromo-4-iodobenzene, $Pd(PPh_3)_4$ (2 mol %), dioxane-H_2O (2:1), Na_2CO_3, reflux.

Scheme 2. Representative Suzuki Coupling Reactions to form $\mathbf{PP_4}$ and $\mathbf{PP_5}$

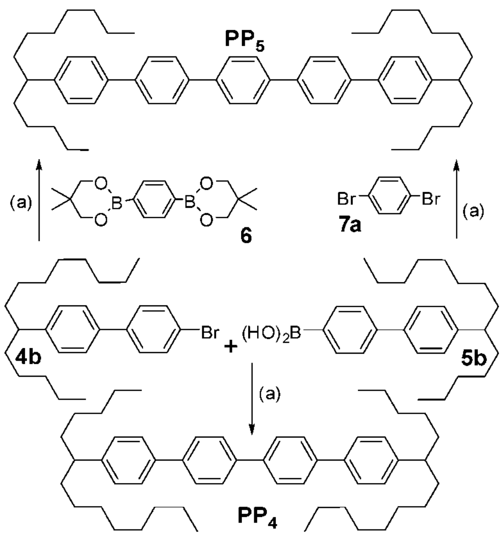

(a) $Pd(PPh_3)_4$ (2 mol %), dioxane-H_2O (2:1), Na_2CO_3, reflux.

were further confirmed by mass spectrometry (see the Supporting Information for the experimental details).

Absorption/Emission Spectroscopy of PP*n*'s. The optical properties of neutral poly-*p*-phenylenes were evaluated with the aid of UV−vis and emission spectroscopy as follows. The electronic absorption spectra of monodisperse poly-*p*-phenylenes, $\mathbf{PP_2}$−$\mathbf{PP_7}$, in dichloromethane, were recorded under conditions of identical concentration (0.1 mM) and temperature (22 °C) and are compiled in Figure 2A. Various poly-*p*-phenylenes showed, unstructured, broad absorption bands that shifted bathochromically with the increasing number (*n*) of phenylene rings from 2 to 7 (see Figure 2A). Although, the molar extinction coefficients of various poly-*p*-phenylenes exhibited a linear increase with the increasing number of phenylene units, corresponding to ~13 000 ± 1000 M^{-1} cm^{-1} per phenylene unit (Table 1, vide infra), the absorption maxima of $\mathbf{PP_2}$−$\mathbf{PP_7}$ did not show a similar linear red-shift with the increasing number of phenylene units. However, a plot of the absorption maxima in energy units (i.e., in wave numbers) versus 1/*n* (where '*n*' is the number of phenylene rings), produces a linear fit (Figure 2B). Linear extrapolation of the curve, results in a value of ~365 nm for the absorption maxima corresponding to a transition energy of ~27 400 cm^{-1} for an infinitely long poly-*p*-phenylene polymer.[21]

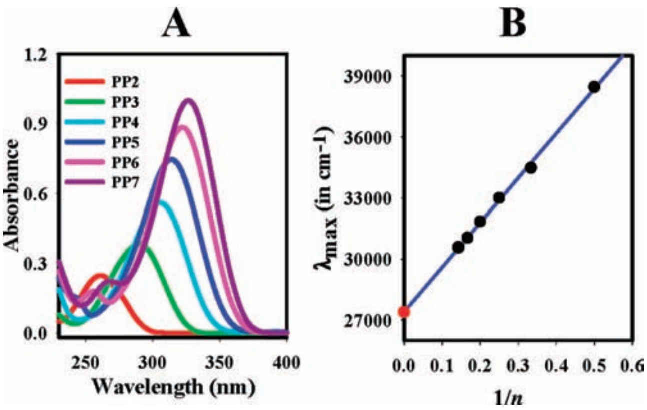

Figure 2. (A) Electronic absorption spectra of 0.1 mM $\mathbf{PP_2}$−$\mathbf{PP_7}$ in dichloromethane at 22 °C. (B) A plot of the λ_{max} in energy units (cm^{-1}) vs 1/*n*, where *n* = number of phenylene rings in a given poly-*p*-phenylene oligomer.

The emission spectra of poly-*p*-phenylenes, recorded as 2.5 × 10^{-7} M solutions in dichloromethane are compared in Figure 3A. The changes in the emission maxima and the relative intensity of emission with increasing number of phenylene units in various poly-*p*-phenylenes are listed in Table 1 (vide infra). The position of emission maxima shift toward the red, and the emission intensities increase with the increasing number of phenylene units. The effect of torsional motion of the phenylene rings is evident from the large Stokes shift of 7598−6165 cm^{-1} (65−80 nm), arising from torsional changes during the transition from the ground to excited states. Furthermore, a plot of the emission maxima, in energy units, versus 1/*n* showed a linear plot (Figure 3B) similar to that observed in Figure 2B for the absorption maxima versus 1/*n* for various poly-*p*-phenylenes.

It is noteworthy that, in contrast to the absorption spectra of various **PP*n***'s in Figure 2, the emission spectra showed a well-defined vibrational structure. The lack of mirror symmetry between the absorption and emission bands is characteristic of π-conjugated hydrocarbons such as poly-*p*-phenylenevinylene, polythiophenes, and poly-*p*-phenylenes in which the effect is ascribed to the larger torsional mobility in the electronic ground state (S^0) in comparison to the first excited singlet state (S^1).[22] Application of ab initio quantum chemical calculations has corroborated this deviation from the Franck−Condon rule as a

---

(21) It is noted that the observed value of 365 nm for the absorption maximum of an infinitely long **PP*n*** in solution, obtained herein, is slightly red-shifted as compared to the reported value of 336 nm for the poly-*p*-phenylene film and may, in part, be due to the difference in the medium employed for the measurements, see:(a) Gin, D. L.; Avlyanov, J. K.; MacDiarmid, A. G. *Synth. Met.* **1994**, *66*, 169–175. (b) Niko, A.; Meghdadi, F.; Ambrosch-Draxl, C.; Vogl, P.; Leising, G. *Synth. Met.* **1996**, *76*, 177–179. (c) Grimme, J.; Kreyenschmidt, M.; Uckert, F.; Mullen, K.; Scherf, U. *Adv. Mater.* **1995**, *7*, 292–295.

Table 1. Optical and Electrochemical Data of Poly-*p*-phenylenes $\mathbf{PP_2}$–$\mathbf{PP_7}$

properties		$\mathbf{PP_2}$	$\mathbf{PP_3}$	$\mathbf{PP_4}$	$\mathbf{PP_5}$	$\mathbf{PP_6}$	$\mathbf{PP_7}$	$\mathbf{PP}_n$[a]
E_{ox1}V vs SCE	V	1.67	1.54	1.49	1.45	1.42	1.41	1.3
λ_{max} (UV–vis)	nm	260	290	305	314	322	326	365
	cm^{-1}	38 461	34 482	32 787	31 847	31 056	30 675	27 400
ε_{max}	$(M^{-1}\ cm^{-1})$	24 631	38 172	55 992	67 723	88 328	91 616	–
λ_{max} (emission)	nm	324	354	378	394	402	408	456
	cm^{-1}	30 864	28 248	26 455	25 381	24 876	24 510	21 900
fluorescence quantum yield	Φ_F	0.2	0.98	1.0	0.98	1.0	1.0	–
fluorescence lifetime	τ (ns)	2.3	2.1	2.0	1.9	1.8	1.6	–
normalized int.		21	242	395	428	497	553	–
$CR^{\bullet+}$, λ_{max}	nm	710	1054	1330	1578	1780	1850	8300
	cm^{-1}	14 085	9487	7518	6337	5618	5408	1200
$CR^{\bullet+}$, ε_{max}	$(M^{-1}\ cm^{-1})$	9500	8376	12 497	13 326	12 392	12 670	–

[a] Note that the last column depicts the predicted values of redox potential and various optical properties for an infinitely long poly-*p*-phenylene, obtained by extrapolation of the curves in various plots (i.e., Figures 2, 3, 5, and 6). As such, the empirical relationship in which the π-electrons are considered as a one-dimensional free electron gas which extends along the length of the oligomer as a particle-in-a-box gives a better fit for the short oligomers but may not necessarily extend to the infinite polymer, owing to saturation phenomenon or breakdown of the $1/n$ relationship due to the localization.[15a,23]

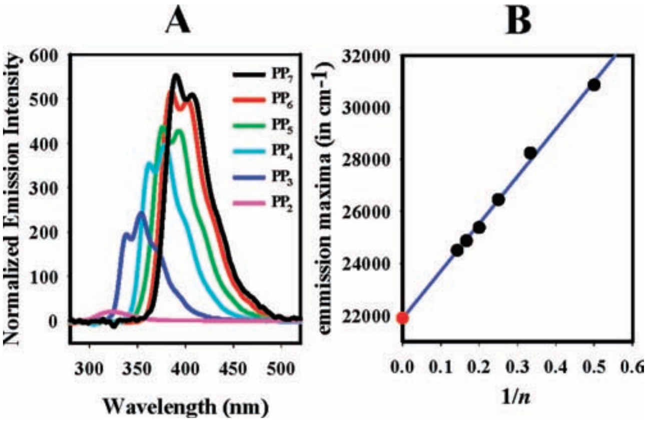

Figure 3. (A) Emission spectra of 2.5×10^{-7} M $\mathbf{PP_2}$–$\mathbf{PP_7}$ in dichloromethane at 22 °C. (B) A plot of the $\lambda_{max,emm}$ in energy units (cm^{-1}) vs $1/n$, where n = number of phenylene rings in a given poly-*p*-phenylene oligomer.

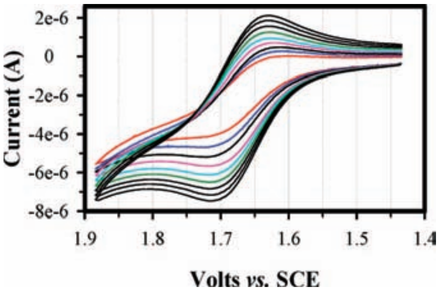

Figure 4. Cyclic voltammograms of 2×10^{-3} M $\mathbf{PP_2}$ in CH_2Cl_2 containing 0.2 M n-Bu_4NPF_6 at scan rates between 100 and 500 mV s^{-1} (with 50 mV increments) at 22 °C.

difference in the structural arrangement in the ground and excited states.[22] Poly-*p*-phenylenes exist in a nonplanar benzenoid form with an interplanar dihedral angle of ~23–40°, and on excitation this ring torsion stiffens due to the contribution of the quinoidal canonical form.

The fluorescence quantum yields for various poly-*p*-phenylenes were also determined using 9,10-diphenylanthracene ($\Phi = 0.91$)[22a] as a standard (see the Supporting Information for the experimental details) and the values are compiled in Table 1. Expectedly, the fluorescence quantum yield for $\mathbf{PP_2}$ ($\Phi = 0.2$) was similar to that of the parent biphenyl[22a] whereas the higher homologues (i.e., $\mathbf{PP_3}$–$\mathbf{PP_7}$) showed close to unity quantum efficiency (see Table 1). The emission lifetimes of $\mathbf{PP_2}$–$\mathbf{PP_7}$ (see the Supporting Information for the experimental details) are compiled in Table 1 and were found to be rather invariant.

Electrochemistry. Next, the redox properties of the poly-*p*-phenylenes were evaluated by subjecting them to electrochemical oxidation at a platinum electrode as a 2×10^{-3} M solution in dichloromethane containing 0.2 M tetra-n-butylammonium hexafluorophosphate (n-Bu_4NPF_6) as the supporting electrolyte. The cyclic voltammograms of various $\mathbf{PP}_n$'s consistently met the reversibility criteria at various scan rates of 100–500 mV s^{-1}, as they all showed cathodic/anodic peak current ratios of $i_a/i_c = 1.0$ (theoretical) at 22 °C, i.e., Figure 4. The reversible oxidation potential of $\mathbf{PP_2}$ was calibrated with ferrocene as an internal standard ($E_{ox} = 0.45$ V vs SCE) and was found to be 1.67 V vs SCE corresponding to the formation of a mono cation radical.

Except the biphenyl and the terphenyl analogue (i.e., $\mathbf{PP_2}$ and $\mathbf{PP_3}$), both of which only show one single reversible oxidation wave, the higher homologues all show two oxidation waves, with the second being quasi-reversible in nature (see Figure 5 and Figure S1 in the Supporting Information). The first oxidation potentials, compiled in Table 1, decrease exponentially with an increase in the number of repeating phenylene units. A quantitative relationship of the oxidation potentials with the number of phenylene rings in various polyphenylenes gives an equation of the form: E_{ox} (V vs SCE) $= 1.3 + 0.74/n$. The slope from the equation for linear fit of the curve between E_{ox} and $1/n$ is a quantitative measure of the effective conjugation. Furthermore, a linear extrapolation of the curve in Figure 5B, results in a value of ~1.3 V vs SCE for the oxidation potential of an infinitely long poly-*p*-phenylene polymer.[23]As such, the lowering of the oxidation potentials with increasing number of phenylene

---

(22) (a) Momicchioli, F.; Bruni, M. C.; Baraldi, I. *J. Phys. Chem.* **1972**, *76*, 3983–3990. (b) Karabunarliev, S.; Baumgarten, M.; Bittner, E. R.; Mullen, K. *J. Chem. Phys.* **2000**, *113*, 11372–11381. (c) Karabunarliev, S.; Bittner, E. R.; Baumgarten, M. *J. Chem. Phys.* **2001**, *114*, 5863–5870. (d) Gierschner, J.; Mack, H.-G.; Luer, L.; Oelkrug, D. *J. Chem. Phys.* **2002**, *116*, 8596–8609. (e) Heimel, G.; Daghofer, M.; Gierschner., J.; List, E. J. W.; Grimsdale., A. C.; Mullen, K.; Beljonne, D.; Bredas, J.-L.; Zojer, E. *J. Chem. Phys.* **2005**, *122*, 054501/1–054501/11.

(23) (a) Compare: Zotti, G.; Schiavon, G.; Berlin, A.; Pagani, G. *Chem. Mater.* **1993**, *5*, 620–624. (b) Hutchison, G. R.; Zhao, Y.-J.; Delley, B.; Freeman, A. J.; Ratner, M. A.; Marks, T. J. *Phys. Rev. B: Condens. Matter* **2003**, *68*, 035204/1–035204/13. (c) Zade, S. S.; Bendikov, M. *Org. Lett.* **2006**, *8*, 5243–5246.

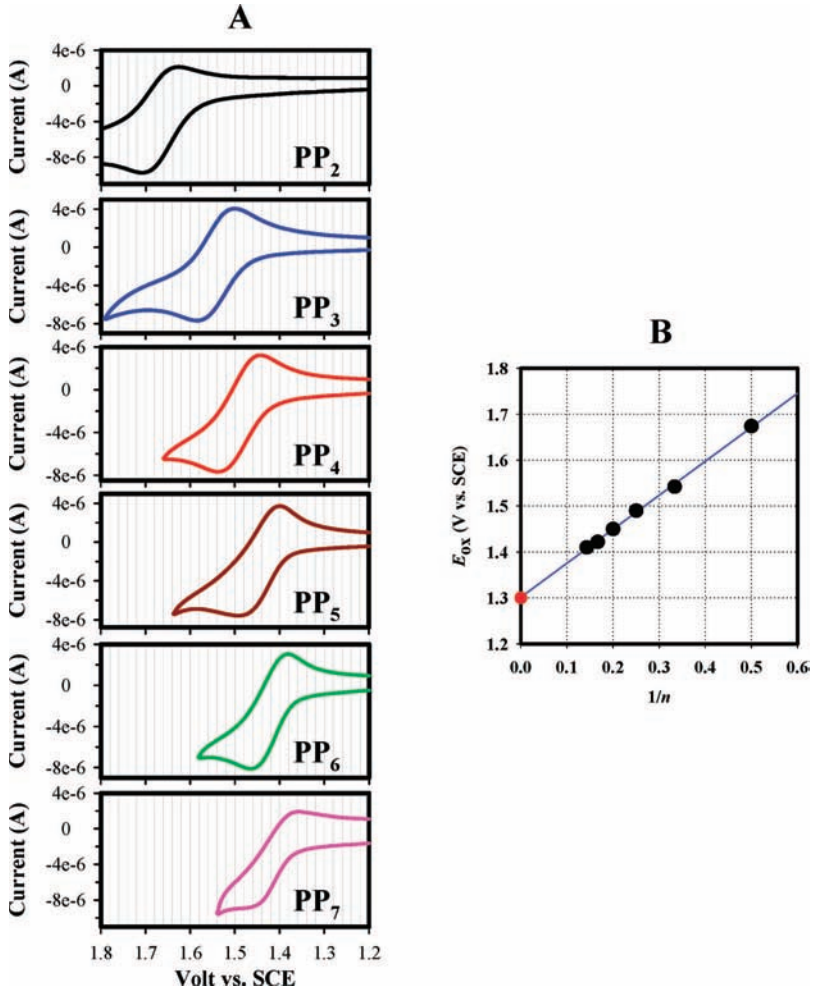

Figure 5. (A) Cyclic voltammograms of 2 × 10^{-3} M $\mathbf{PP_2}$−$\mathbf{PP_7}$ in CH_2Cl_2 containing 0.2 M *n*-Bu_4NPF_6 at a scan rate of 200 mV s^{-1} at 22 °C. (B) A plot of the oxidation potentials (E_{ox1}) vs 1/*n*, where *n* = number of the phenylene rings in various poly-*p*-phenylene oligomers $\mathbf{PP_2}$−$\mathbf{PP_7}$.

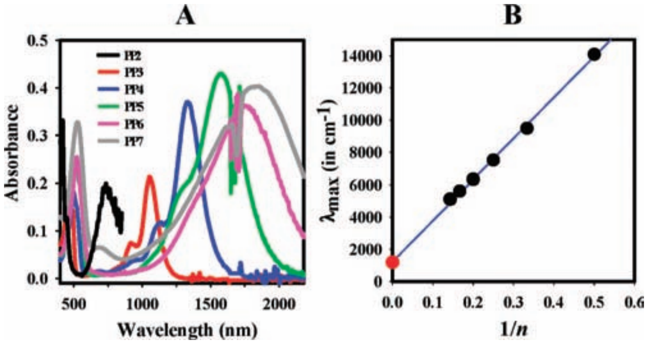

Figure 6. (A) Cation radical spectra of oligomers $\mathbf{PP_2}$−$\mathbf{PP_7}$ (1 × 10^{-5} M) in dichloromethane at 22 °C. Note that the $\mathbf{PP_2}$ cation radical (black curve) was generated via laser-flash photolysis, see text. (B) A plot of the λ_{max} in energy units (cm^{-1}) vs 1/*n*, where *n* is the number of phenylene rings in various $\mathbf{PP}_{\boldsymbol{n}}$ oligomers. Note that the glitches in the absorption spectra at ~1700 nm arise due to the somewhat poor subtraction of the absorption bands due to the solvent.

units, in first approximation, represents the rise of the HOMO levels. It may also be noted that the reduction of the band gap in poly-*p*-phenylenes (as well as other conducting polymers) results mainly from an increase in the HOMO levels. In this context, it is noteworthy that the optical band gap calculated from the absorption edge of the UV−vis absorption spectra using the formula ΔE_{opt} (eV) = hc/λ_{onset} also follows the similar 1/*n* dependence and an extrapolation of the ΔE_{opt} vs 1/*n* curve provides a value for the optical band gap of 2.9 eV for an infinitely long poly-*p*-phenylene polymer. Thus, a demonstration of 1/*n* dependence of redox potentials as well as various optical properties of neutral and cation radicals with systematic increase of the repeating units (such as phenylenes in poly-*p*-phenylenes) serves to provide an estimate of the band gap and other optoelectronic properties of the infinite-chain polymers.

Generation of the $\mathbf{PP}_{\boldsymbol{n}}$ Cation Radicals and their Electronic Spectroscopy. The inverse relationship of the optical and redox properties of poly-*p*-phenylenes $\mathbf{PP_2}$−$\mathbf{PP_7}$, with the increasing number of repeating units, prompted us to determine how the optical transitions in their cation radicals will vary with the increasing number of phenylene rings. The reversibility of the first oxidation potentials of various poly-*p*-phenylene oligomers suggested that their cation radicals should be sufficiently stable, and may be generated using nitrosonium hexachloroantimonate (NO^+ $SbCl_6^-$)[24] as an oxidant. Indeed, when a 1 × 10^{-5} M solution of poly-*p*-phenylene oligomer $\mathbf{PP_3}$, in dichloromethane, was exposed to a 1 × 10^{-5} M solution of NO^+ $SbCl_6^-$, in dichloromethane, at ambient temperature and under strict exclusion of oxygen, an orange-red solution of $\mathbf{PP_3}$ cation radical was produced, i.e., eq 1.

---

[24] Rathore, R.; Burns, C. L. *J. Org. Chem.* **2003**, *68*, 4071–4074.

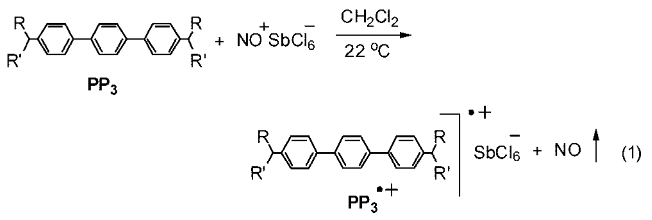

The nitric oxide gas generated in the reaction in eq 1 was entrained by bubbling argon through the solution. The resulting solution of the **PP$_3$** cation radical was stable for several hours at ~0 °C as judged by the lack of changes in the UV−vis absorption spectra.[25] Similarly, the vividly colored cation radical solutions of **PP$_4$**−**PP$_7$** were prepared and their electronic absorption spectra are compared in Figure 6A. The reaction of **PP$_2$** (E_{ox} = 1.67 V vs SCE) with NO$^+$ was highly endergonic and therefore, its cation radical was generated using laser-flash photolysis as follows. A diffusional electron-transfer quenching of the photoexcited chloranil triplet as an oxidant (E_{red} = 2.2 V vs SCE)[26] with **PP$_2$** produced a characteristic cation radical spectrum together with the absorption bands due to the chloranil anion radical as shown in Figure 6A (black curve).[26] Similarly, the cation radical spectra of representative **PP$_n$** derivatives (such as **PP$_4$** and **PP$_6$**) were also produced via the laser-flash photolysis technique and were found to be similar to those obtained via NO$^+$ oxidation (see Figures S2 and S3 in the Supporting Information). The absorption maxima of various cation radicals together with the other optical and electrochemical data of **PP$_2$**−**PP$_7$** are compiled in Table 1.

A comparison of the cation radical spectra of **PP$_2$**−**PP$_7$** (in Figure 6A) showed that they all contained a highly characteristic twin absorption band[27] that shifted red from 710 (14 085 cm^{-1}) to 1850 nm (5406 cm^{-1}) going from **PP$_2$** to **PP$_7$** (Table 1). Furthermore, in Figure 6B, a plot of the absorption maxima of the **PP$_2$**−**PP$_7$** cation radicals in energy units (cm^{-1}) versus 1/*n* (where *n* is number of phenylene units) showed a linear relationship akin to those observed in Figures 2, 3, and 5. A linear extrapolation of the curve in Figure 6B results in a value of ~1200 cm^{-1} for the absorption maxima for the cation radical of an infinitely long poly-*p*-phenylene polymer.

X-ray Crystallography of the Quaterphenyl Cation Radical. It is believed that a single charge in biphenyl-type cation radicals is stabilized largely by quinoidal valence-bond resonance, as shown in Scheme 3. Such a resonance stabilization of **PP$_2$**$^{+\bullet}$ requires that both the phenylene units lie coplanar with respect to each other. Indeed the remarkable similarity of the absorption spectra of **PP$_2$**$^{+\bullet}$−**PP$_7$**$^{+\bullet}$ in Figure 6A would suggest that the hole is most likely stabilized in each case by a similar quinoidal charge resonance, i.e., Scheme 3.[28]

Scheme 3

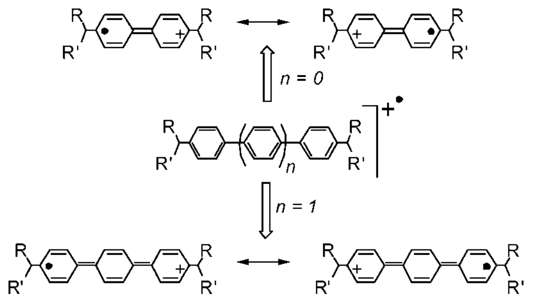

The valence-bond resonance structures of **PP$_2$**$^{+\bullet}$ and **PP$_3$**$^{+\bullet}$, depicted in Scheme 3, require that the phenylene moieties adapt a coplanar conformation with respect to each other in order to effectively stabilize the cationic charge. Isolation and X-ray structure determination of a cation-radical salt of a quaterphenyl derivative (**PP$_4'$**), having *tert*-butyl solubilizing groups at the terminal positions,[17] have indeed unequivocally established that a single charge is delocalized via a quinoidal distortion of the central phenylene rings (see Figure 7). The salient features of the molecular structure of **PP$_4'$**$^{+\bullet}$are summarized as follows.

(i) The central bond distance of 1.440 Å between the two inner benzene rings B and C in **PP$_4'$**$^{+\bullet}$ is considerably shorter than the two peripheral C−C bonds between the outer rings and the penultimate ones (i.e., 1.454 Å between rings A and B and 1.463 Å between rings C and D). This represents a contraction of the central C−C bond (between ring B and C) by 5 pm in the oxidized form in comparison to 1.1 pm in neutral

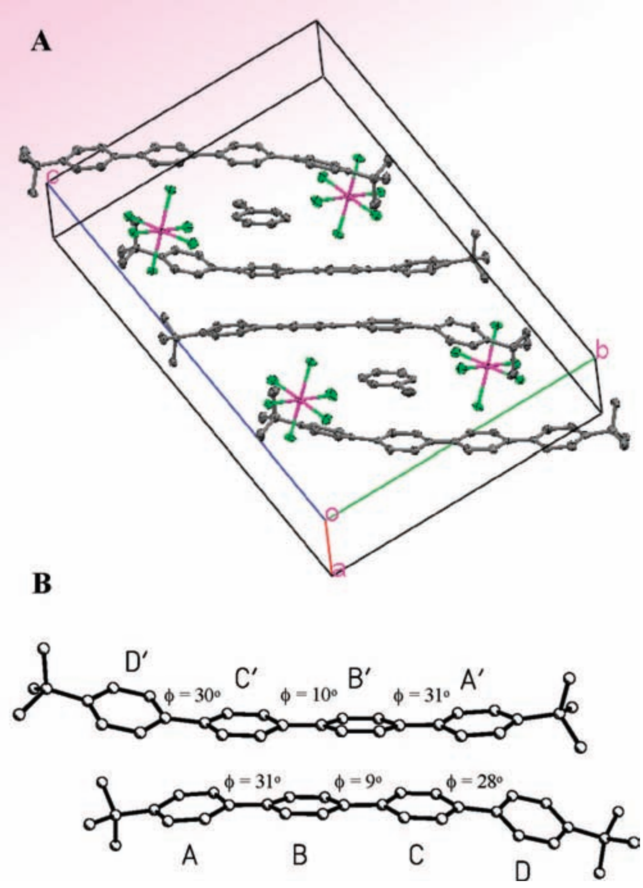

Figure 7. Crystal structure of **PP$_4'$**$^{+\bullet}$ SbCl$_6^-$ cation radical with the packing diagram showing that the toluene molecules are embedded between the stacked dimeric pairs (A) and the labeling scheme for the phenylene rings in the dimeric pair (B).

---

[25] Note that the addition of excess **PP$_3$** donor (up to 5 equiv) to the solution of **PP$_3$**$^{+\bullet}$ or increasing the concentration of **PP$_3$**$^{+\bullet}$ by 10-fold did not show any change in its absorption spectrum.

[26] (a) Rathore, R.; Hubig, S. M.; Kochi, J K. *J. Am. Chem. Soc.* **1997**, *119*, 11468–11480. (b) Hübig, S. M; Rathore, R.; Kochi., J K. *J. Am. Chem. Soc.* **1999**, *121*, 617–626.

[27] (a) The position of the high energy band is similar to those previously reported for the biphenyl and terphenyl cation radicals by a laser-flash photolysis method. See: Khanna, R. K.; Jiang, Y. M.; Creed, D. *J. Am. Chem. Soc.* **1991**, *113*, 5451–5453. (b) Khanna, R. K.; Jiang, Y. M.; Srinivas, B.; Smithhart, C. B.; Wertz, D. L. *Chem. Mater.* **1993**, *5*, 1792–1798. (c) Rubio, M.; Merchan, M.; Orti, E. *J. Phys. Chem.* **1995**, *99*, 14980–14987. (d) Shida, T. *Electronic Absorption Spectra of Radical Ions*; Elsevier: Amsterdam, 1988.

$\mathbf{PP}_4'$. (ii) The longitudinal bonds inside the rings are contracted, whereas the transverse bonds are lengthened in comparison to neutral $\mathbf{PP}_4'$, indicative of a quinoidal bond alteration.[29] In numerical terms, the longitudinal bond contraction results in bond lengths of 1.377 (ring A), 1.362 (ring B), 1.368 (ring C), and 1.381 Å (ring D) from an average of 1.38 Å in the neutral $\mathbf{PP}_4'$ and a consequent lengthening of the transverse bonds to 1.397/1.409 (ring A), 1.419/1.424 (ring B), 1.421/1.413 (ring C), and 1.407/1.399 Å (ring D). The magnitude of the bond contractions and expansions reaches a maximum in the inner rings while the peripheral rings are less affected. (iii) The torsional angles (ϕ) between the rings A/B/C are $\sim$0.1−15°, resulting in a nearly coplanar conformation. However, for the peripheral ring D, this angle slightly increases, primarily due to the steric hindrance of the *t*-butyl group of the adjacent stacked molecule. Thus, the formation of the cation radical smoothes out the torsional motion of the interconnected aryl rings from their typical values of $\sim$30° between the outer rings and $\sim$10° between the central rings as in the neutral form, in order to allow effective stabilization of the cationic charge by quinoidal distortions.[29] (iv) Considering the magnitude of quinoidal distortion to be a linear function of the amount of charge allocated within the corresponding ring, we can estimate that rings A−D bear the following positive charges: 0.15 (A), 0.46 (B), 0.33 (C), and 0.06 e^- (D). As such, the asymmetric charge distribution further attests to the strong electronic coupling within the "shifted" dimeric associates.[30]

These salient features of the $\mathbf{PP}_4'$ cation radical can only be rationalized when one considers that the single charge is stabilized by a quinoidal valence bond resonance structure (i.e., Scheme 3). Such a resonance form having a quinoidal structure leads to unequal bond distortions in the aryl rings as well as planarization of the aryl rings for effective π-conjugation with the magnitude of changes being the highest in the central rings.

Summary and Conclusions

In summary, we have successfully synthesized a well-defined series of poly-*p*-phenylene oligomers containing up to eight phenylene moieties with branched alkyl (i.e., 6-tetradecyl) groups as the end-capping substituents. Despite having long branched alkyl chains as the solublizing groups, the solubility of poly-*p*-phenylene oligomers beyond seven phenylene units decreases sharply. All electronic and optoelectronic properties of poly-*p*-phenylenes, containing up to seven phenylene moieties (i.e., $\mathbf{PP}_2$−$\mathbf{PP}_7$), follow a 1/*n* relationship (where *n* is number of phenylene moieties) with the increasing number of phenylene moieties. The low-energy electronic transitions of the $\mathbf{PP}_2$−$\mathbf{PP}_7$ cation radicals generated either by laser-flash photolysis or by chemical oxidation using nitrosonium hexachloroantimonate as an oxidant also varied according to the familiar inverse (1/*n*) relationship. The isolation and X-ray crystallographic characterization of a representative cation-radical salt of a quaterphenyl derivative allowed us to demonstrate that a single charge in $\mathbf{PP}_n$ cation radicals is stabilized via a quinoidal distortion of the central phenylene rings, which requires planarization of the central phenylene rings. Thus, the observed inverse relationship of bathochromic shifts of the cation radical transitions, as well as all measured electronic and optoelectronic properties against the increasing number of phenylene units in various $\mathbf{PP}_n$'s, suggests that the effective conjugation length in poly-*p*-phenylenes is controlled by the increasing number of interactions of ortho hydrogens which prevent simultaneous planarization of continuous arrays of a large number of phenylene moieties. It is further emphasized that the simultaneous planarization of a large continuous array of phenylene moieties in poly-*p*-phenylenes affects all properties, i.e., optical (Figures 2 and 6), photoluminescence (Figure 3), and redox (Figure 5), in a similar way. Studies are underway for a comprehensive investigation of the optoelectronic properties of a series of completely planar poly-*p*-phenylene derivatives and comparison with the $\mathbf{PP}_n$ derivatives described above, and these findings will be reported in due course.

Acknowledgment. We thank the National Science Foundation (Career Award) for the financial support and Sergey V. Lindeman (Marquette University) for X-ray crystallography.

Supporting Information Available: General experimental methods, synthetic procedures, ^{1}H/^{13}C NMR spectra of various compounds, cyclic voltammograms, the transient spectra of the representative $\mathbf{PP}_n$ cation radicals, the ORTEP diagrams, and the X-ray crystallographic data for $\mathbf{PP}_4'$. This material is available free of charge via the Internet at http://pubs.acs.org.

JA805102D

---

(28) (a) Rubio, M.; Mercha′n, M.; Orti′, E. *J. Phys. Chem.* **1995**, *99*, 14980–14987. (b) Porter, W. W.; Vaid, T. P. *J. Org. Chem.* **2005**, *70*, 5028–50235. (c) Peart, P. A.; Repka, L. M.; Tover, J. D. *Eur. J. Org. Chem.* **2008**, 2193−2206. (d) Also see:Tolbert, L. M. in ref 15a.

(29) (a) Rubio, M.; Merchán, M.; Ortí, E. *J. Phys. Chem.* **1995**, *99*, 14980–14987. (b) Brédas, J. L.; Thémans, B.; André, J. M. *Phys. Rev. B* **1982**, *26*, 6000–6002.

(30) (a) The cation radical dimer pair in solid state is most likely stabilized via a charge-resonance process, i.e., $\mathbf{PP}_4{}^{+\bullet} + \mathbf{PP}_4{}^{+\bullet} \leftrightarrow \mathbf{PP}_4{}^{++} + \mathbf{PP}_4$. For example, see:(b) Kochi, J. K.; Rathore, R.; Le Magueres, P. *J. Org. Chem.* **2000**, *65*, 6826–6836.